Choline chloride–formic acid mixture as a medium for the reduction of pertechnetates – electrochemical and spectroscopic studies†

Damian Połomski,[a] Nicole A. DiBlasi,[b] Kathy Dardenne,[b] Xavier Gaona,[b] Kenneth Czerwinski[c] and Maciej Chotkowski *[a]

The physicochemical properties of a choline chloride (ChCl) and formic acid (FA) mixture (1 : 2 molar ratio) have been studied over a broad range of temperatures (−140 to 60 °C). Differential scanning calorimetry has shown that the examined system remains in the liquid state at very low temperatures – a glass transition is observed in the range of −125 °C to −90 °C. The kinematic viscosity, ionic conductivity and the width of the electrochemical window determined for this system revealed its beneficial electrochemical properties. This indicates the suitability of ChCl : FA electrolytes in electrochemical measurements. In this non-aqueous electrolyte, electrochemical reduction of Tc(VII) ions has been studied for the first time. Cyclic voltammetry and chronopotentiometry experiments revealed that the electroreduction of pertechnetates is a multi-path process which leads to the formation of a Tc(IV) ionic form. X-Ray absorption spectroscopy of the latter revealed its structure as a $TcCl_6^{2-}$ complex.

A Introduction

Choline-based non-aqueous solutions are promising solvents which are suitable for electrochemical studies of numerous redox systems.[1–3] These relatively new liquid solutions are used for electrodeposition of various elements and their alloys, such as Ru, Pd, and Ni–Fe.[4–6] One of the most often studied non-aqueous choline-based solutions is a mixture of choline chloride and urea (ChCl : U) with a molar ratio of 1 : 2. This is a room temperature liquid eutectic which exhibits a high viscosity of *ca.* 950 cP (25 °C) and a relatively low ionic conductivity of 1 mS cm^{-1} (25 °C).[7] A mixture of choline chloride with ethylene glycol is another very common choline based deep eutectic solvent. As compared to ChCl : U, this liquid reveals a lower viscosity (*ca.* 50 cP at 25 °C) and a higher ionic conductivity (*ca.* 8 mS cm^{-1} at 25 °C).[8]

Choline based salts may act as hydrogen bond acceptors and their mixtures with hydrogen bond donors (*e.g.*, carboxylic acids, urea) reveal several unique properties. As an example, the processes taking place during cooling of these liquids is sometimes described as a glass transition leading to the formation of an amorphous phase.[1] Another very interesting property of non-aqueous mixtures containing ChCl is their ability to dissolve transition metal oxides. For instance, Abbot *et al.*[9] reported that a mixture containing ChCl and malonic acid (1 : 2 molar ratio) dissolves manganese oxide with the generation of a $MnCl_3^-$ complex. The solubility of MnO_2 is several times higher in choline chloride : oxalic acid solutions than in 1.8 M oxalic acid : water solutions.[10]

Choline acetate (ChA) systems have also been studied (ChA). In our previous paper,[11] we showed that solutions containing ChA in FA and AA (acetic acid) exhibit significantly lower viscosity and higher ionic conductivity than the ChCl : U system under the same conditions. The conductivity of ChA : FA and ChA : AA systems is also higher than that of the respective pure carboxylic acids.

Choline based solutions with a low water content are very attractive electrolytes in studies of species which are highly sensitive to processes driven by the presence of water, *e.g.* hydrolysis or disproportionation. Apart from relatively low viscosity and high conductivity, they are able to form complexes which stabilize certain oxidation states of various radioactive elements, for example uranium(V).[12] It follows then that such solutions are very promising electrolytes for studies on redox reactions of Tc. This element is one of the most important radionuclides both for nuclear medicine and the nuclear industry.[13,14] Ionic forms of Tc are of particular interest to scientists dealing with the synthesis of radiopharmaceuticals[15] or specialists in the field of the nuclear industry, *e.g.* separation processes of Tc from spent nuclear fuel.[16]

[a] *University of Warsaw, Faculty of Chemistry, Biological and Chemical Research Centre, Żwirki i Wigury 101, 02-089, Warsaw, Poland. E-mail: mchotk@chem.uw.edu.pl*

[b] *Karlsruhe Institute of Technology, Institute for Nuclear Waste Disposal, Hermann-von-Helmholtz-Platz 1, Eggenstein-Leopoldshafen, 76344, Germany*

[c] *Radiochemistry Group, University of Nevada, Las Vegas, NV, 89154, USA*

† Electronic supplementary information (ESI) available.

Recent times have witnessed strong interest in practical applications of Tc isotopes. Although this element has been known since 1937, its redox chemistry is still far from fully understood. This is due to the fact that the redox reactions of Tc in aqueous solutions are very complex and affected by side reactions, such as hydrolysis, disproportionation and/or polymerization.[17,18] Our previous spectroelectrochemical studies on the reduction of Tc(VII) discussed the formation of ionic Tc(V) species in highly acidic aqueous electrolytes.[19] These species were also observed by other authors.[20,21] In a less acidic environment, the dominant reduced forms of Tc are Tc(III/IV) structures or hydrated Tc(IV) oxide, while Tc(V) quickly disproportionates.[17] Ionic species containing reduced Tc may form various structures. For instance, Vichot *et al.*[22] reported the generation of polyoxopolymetallic species in chloride/sulfate solutions. In turn, Rajec and Macášek[23] reported the formation of hexachlorotechnetates(IV) as a result of electrochemical reduction of $TcOCl_5^{2-}$ ions in 4 M HCl_{aq}. In more concentrated hydrochloric acid solutions, other Tc complexes ($Tc_2Cl_8^{2-}$) are observed.[24] Dimeric Tc species are reported to be generated in concentrated aqueous formate[25–27] or acetate[28] solutions.

In contrast to aqueous electrolytes, there are only a handful of papers which focus exclusively on electrochemical characteristics of reduced Tc in non-aqueous electrolytes.[17] The latter are especially attractive because they allow for the avoidance of numerous side reactions that include water, such as hydrolysis, disproportionation and the formation of poorly soluble TcO_2. It is expected that the application of choline salt : carboxylic acid mixtures allows for eliminating the formation of oxide containing Tc(IV) species due to complexing properties of choline cations. Furthermore, autodissociation of the acid leads to the formation of H^+, whose presence is beneficial for the reduction of pertechnetates. This manuscript reports for the first time the results of studies on the electrochemical reduction of Tc(VII) in a choline chloride–formic acid solution.

B Experimental

Caution! Technetium-99 is a long-lived beta emitter (E_{max} = 293 keV). Although radiation from small amounts of its salt is relatively low (activity: 629 kBq per 1 milligram of Tc-99), all operations must be carried out in specially equipped laboratories to avoid contamination or ingestion.

Materials

Choline chloride and choline acetate (reagent grade, ≥98%) were purchased from IoLiTec. Tin chloride ($SnCl_2{\cdot}2H_2O$; reagent grade 98%) was delivered by Sigma Aldrich. Formic acid (98–100%, for analysis) was purchased from Merck. The mixtures of ChCl and FA with a molar ratio of 1 : 2 were prepared by dissolution of respective amounts of this salt in formic acid.[11]

Methods

The thermal properties of ChCl : FA mixtures were determined using differential scanning calorimetry (Mettler Toledo DSC 1, STARe). Each sample (*ca.* 15–40 mg) was placed in a tightly sealed aluminum pan. The measurements were performed at a scan rate of 5 K min^{-1} in the temperature range from −140 °C to 20 °C. The DSC system was calibrated with a 99.9999% purity indium metal sample. The water content of the mixtures was measured using a TitriLine KF – Coulomat AG (Schott Instruments). Important physical parameters of this liquid were determined in the temperature range ranging from 25 °C to 60 °C. The density (ρ) was measured using a Gay-Lussac pycnometer (Carl Roth GmbH, volume 1.029 mL) and a precise laboratory balance (RADWAG PS 210/C/2). The kinematic viscosity (ν) of the samples containing the ChCl : FA mixture was measured using an Ubbelohde viscometer (Carl Roth GmbH) while their dynamic viscosity (η) was analyzed using a rotational viscometer (Brookfield DV-II+ Viscometer). The ionic conductivity (κ) was determined using a conductivity cell (ECF-1 t 0429/19) coupled with a conductivity meter (Elmetron CX-401). The electrochemical measurements were performed using an Autolab (PGSTAT128N) electrochemical analyser. The UV-vis spectra were recorded using a MultiSpec 1500 (Shimadzu) spectrophotometer. All of the electrochemical measurements were carried out in a three-electrode system with platinum acting as a counter electrode and silver serving as a reference electrode. Its potential (measured at an open circuit potential) *vs.* saturated calomel electrode was −235 mV at 25 °C. All potentials in the text are referred to as the Ag electrode. The working electrode was made of a glassy carbon rod. A rotating disc electrode (RDE) with a glassy carbon disk in a Teflon sleeve (RDE AFE5T050GC) was used in electrochemical experiments carried out under hydrodynamics conditions. The diffusion coefficient of the pertechnetates in the choline-based solutions was calculated according to the procedure described previously.[29] The samples containing pertechnetates were prepared by direct dissolution of potassium or sodium pertechnetate in ChCl : FA. $K^{99}TcO_4$ was provided by the Helmholtz-Zentrum Dresden-Rossendorf (Germany). Tc in the form of $Na^{99}TcO_4$ was supplied by Karlsruhe Institute of Technology. A literature review[17] reveals that the identity of the alkali counter ion (Na^+ or K^+) has no influence on the reduction of the pertechnetates.

The concentration of $^{99}TcO_4^-$ in the solutions was determined using liquid scintillation counting (PerkinElmer Tricarb 2910 TR). Two liquid solutions containing Tc were prepared for the XAS experiments. The first one (solution in sample I) contained 3 mM of $NaTcO_4$ dissolved in ChCl : FA. The solution in sample II was prepared to target already reduced Tc species, and was prepared using $SnCl_2$ as a reducing agent. It was prepared by mixing 0.2 mL of ChCl : FA solution containing Sn(II) ions with 2 mL of 3 mM TcO_4^- in ChCl : FA. The Sn(II) solution was prepared by dissolving 50 mg of $SnCl_2{\cdot}2H_2O$ in 3 mL of ChCl : FA solution. This mixture was stirred for 30 minutes and was then centrifuged (6000 rpm) for 10 min.

Following centrifugation, 0.2 mL of the supernatant was added to the solution containing the pertechnetates. Before starting the experiments, the solutions in samples I and II were stored in a glovebox under a nitrogen atmosphere for 3 weeks. X-Ray absorption spectroscopy (XAS) measurements were conducted at the INE-Beamline for Actinide Research[30,31] at the KIT light source (KARA storage ring, KIT Campus North), where the storage ring was operated at 2.5 GeV electron energy with a mean electron current of 120 mA. Spectra were recorded in both fluorescence and absorbance detection modes using an 8-pixel LEGe solid-state detector and argon-filled ionization chambers, while incident beam intensity and the transmission of a reference 20 μm molybdenum (Mo) metal foil were recorded using inert gas-filled ionization chambers at ambient pressure. Aqueous samples were prepared by transferring ~250 μL of experimental solution into polyethylene vials within a fume hood. The vials were subsequently sealed with Parafilm™ and mounted using Kapton® tape into a gas-tight cell within an argon glovebox. Doubly contained samples were then transported to the INE-beamline for analysis. During XAS measurements, argon was continuously flushed through the sample cell, ensuring the presence of an inert atmosphere and gas-tight secondary sample containment, and 3–6 scans were collected for each sample. The XANES data reduction was performed with the ATHENA software from the Demeter 0.9.26 program package following standard procedures.[32] Technetium spectra were calibrated against the first inflection point within Mo K-edge (20 000 eV) reference spectra and averaged to reduce statistical noise. The E_0 for each experimental spectrum was selected at the first inflection point of the white line by using the first derivative. The TcO_2(am,hyd) and TcO_4^- reference spectra were collected at the INE-beamline under similar experimental conditions and treated to similar data analysis procedures. The EXAFS data analysis was based on standard least squares fit techniques: FEFFIT code (FEFF6) within the Demeter program package was used to determine neighbor atom distances (R_i), Debye–Waller factors (σ_i^2), and coordination numbers (N_i) for different coordination shells (i), all used to derive *ab initio* scattering amplitudes and phase shifts. The $TcCl_4$(s) crystallographic information file (COD: 4329921) was obtained from Johnstone *et al.*[33] and used for FEFF/ATOMS calculations. All fit operations were performed in -s*R*pace with a fixed amplitude reduction factor (S_0^2 = 0.95) previously determined through TcO_4^- reference spectrum fitting with N_O fixed to 4.0.

C Results and discussion

Fig. 1 shows the results of differential scanning calorimetry recorded for ChCl : FA solutions at a heating rate of 5 °C min^{-1}. No processes are observed during cooling from room temperature *ca.* −90 °C for this mixture and at this heat rate (ESI† S1). When the temperature is reduced to −90 to −125 °C, changes in heat flow are observed for both freshly prepared and 1 year aged samples. The shape of the DSC curves in this temperature range is typical for a transition of an amorphous material from a brittle state to a viscous state (Fig. 1). The glass transition points (curve midpoint) are observed at almost the same temperature of −109.2 °C and −108.5 °C for the freshly prepared and the aged sample, respectively (ESI† S1). It should be noted that the transition temperature is more than 60 °C lower than the lowest value of the freezing point reported for the FA-water solutions.[34]

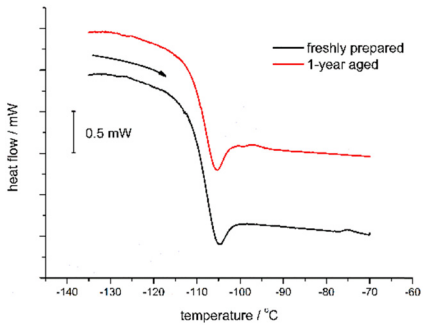

Fig. 1 DSC thermograms recorded for ChCl : FA (1 : 2 molar ratio), freshly prepared and 1 year aged samples, in the temperature range from −135 °C to −70 °C, heat rate = 5 K min^{-1}.

Other physicochemical properties of the analysed ChCl : FA solution measured at the temperature range 25 to 60 °C are summarized in Table 1. The results are comparable to those previously reported for other choline-based carboxylic acid systems.[11] In this paper, we discussed the time variation of the water content (w%$_{H_2O}$) of choline based:carboxylic acid solutions. It was found that formic acid and choline cation (containing a hydroxylic group) undergo an esterification reaction. This is an equilibrium process and the water content in this mixture stabilizes within 3 weeks at a level of 3.4%. This indicates that drying of the mixture will not completely remove water because the latter is generated in the esterification process. The density of ChCl : FA solvent is slightly higher than 1.1 g cm^{-3}. The values of the viscosity, as well as the ionic conductivity, are in the range of 8–21 cSt and 14–21 mS cm^{-1}, respectively. It follows that the temperature variations of ν and κ of ChCl : FA solutions are significantly smaller than for choline chloride : urea[7] or choline chloride dissolved in oxalic, malonic or citric acid.[35] Moreover, the viscosity of the ChCl : FA

Table 1 Kinematic viscosity (ν), density (ρ), and conductivity (κ), at various temperatures of ChCl : FA mixture (1 : 2 molar ratio; after 3 weeks of synthesis)

Temp.[a] (°C)	ν^b (cSt)	ρ^c (g cm^{-3})	κ^d (mS cm^{-1})
25[e]	21.12	1.155	14.60
30	17.55	1.152	15.90
35	15.28	1.148	16.48
40	13.32	1.145	17.43
45	11.38	1.141	18.16
55	9.10	1.135	19.65
60	8.12	1.131	20.67

Uncertainties. [a] $u(T)$ = ±0.05 °C. [b] $u(\nu)$ = 5%. [c] $u(\rho)$ = ±0.8%. [d] $u(\kappa)$ = ±0.05 mS cm^{-1}. [e] Literature data given from ref. 11.

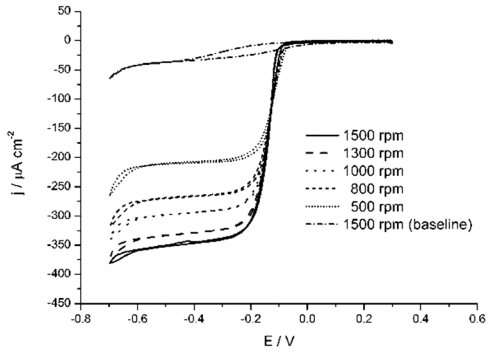

Fig. 2 Cyclic voltammograms recorded in 1.2 mM $KTcO_4$ + ChCl : FA on the glassy carbon rotating disk electrode (RDE) for various rotating rates, T = 25 °C, v = 250 mV min^{-1}.

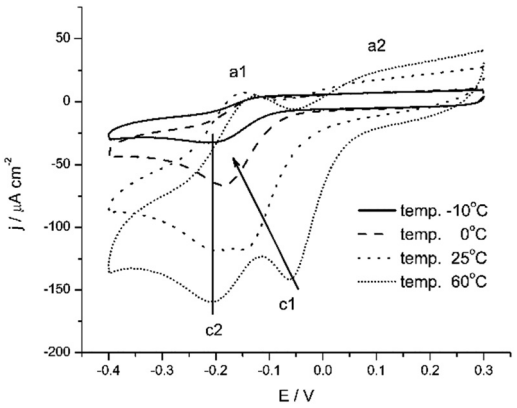

Fig. 3 Cyclic voltammograms recorded for various temperatures in 1.2 mM $KTcO_4$ + ChCl : FA, scan rate of 50 mV s^{-1}.

mixture is lower than for the choline chloride : ethylene glycol mixture. The latter also has a lower ionic conductivity than the ChCl : FA system at the same temperature.

In our previous paper[11] we showed that the temperature dependence of the conductivity and the viscosity of the choline acetate : carboxylic acid mixtures is appropriately described by eqn (1):

$$\ln \alpha = \ln \alpha_0 + \frac{E_\alpha}{RT} \quad (1)$$

where α_0 is a constant, E_α is the activation energy for ionic conductivity (or viscosity), T is the temperature (K), and R is the universal gas constant (8.314 J K^{-1} mol^{-1}). Using eqn (1) and data from Table 1 we estimated values of the respective parameters of the examined ChCl : FA mixtures at temperatures lower than 25 °C. These determined kinematic viscosity and conductivity values were equal to 41 cSt and 11 mS cm^{-1} at 0 °C, respectively (see ESI† S2). It should be stressed that these values are acceptable for the electrochemical measurements. Furthermore, the ChCl : FA system does not undergo any electrochemical reactions below 0.3 V (ESI† S3). Fig. 2 shows the results of voltammetric measurements carried out under hydrodynamic conditions. The electroreduction of pertechnetates is observed at potentials lower than −0.1 V. This reaction is diffusion limited and leads to the formation of well-developed limiting current observed for all rotating rates. A linear relationship between the reciprocal of the current density (j^{-1}) and the reciprocal of the square root of the rotation rate ($\omega^{-1/2}$) is observed (ESI† S4) and this allows application of the Koutecky–Levich equation[36] for further analysis of the results. The calculated number of electrons involved in the electroreduction of Tc(VII) is equal to 3.1 ± 0.2. This result indicates that Tc(IV) is the final product of the pertechnetate electroreduction. As will be shown later, the results provided by the hydrodynamic experiments are in line with UV-vis and XAS data recorded for non-hydrodynamic conditions. A review of the literature shows that various deep eutectic solvents reveal significantly different relationships between the shear rate and the dynamic viscosity.[37] Some of these liquids are described as Newtonian fluids in a wide range of temperatures and shear rate values while others, like ChCl : U, behave as non-Newtonian fluids. It is worth mentioning that the largest changes in the viscosity are observed usually for low shear rate values (below 1 s^{-1}). In order to determine the rheological properties of the ChCl : FA system additional experiments aimed at the determination of viscosity of this liquid were performed (ESI† S5). The measurements were carried out for shear rates higher than 0.01 s^{-1} and it follows that this dynamic viscosity of the ChCl : FA mixture is not affected by this parameter. This indicates that the influence of ω on the diffusion coefficient of Tc(VII) is meaningless under the experimental conditions applied.

In contrast to the hydrodynamic conditions, the voltammetric curves recorded under stationary conditions reveal two processes. Fig. 3 shows CVs recorded in 1.2 mM Tc(VII) + ChCl : FA (1 : 2 molar ratio) solution at various temperatures from −10 °C to 60 °C. The figure shows a strong temperature impact on the shapes of the voltammetric curves. Their shapes are similar to those previously reported in H_2SO_4 solutions.[29] As an analogy to the processes observed in acidic solutions, the first reduction wave can be related to the electroreduction of pertechnetates to Tc(V). The latter Tc species are transformed to Tc(IV) *via* an electrochemical pathway or chemical (disproportionation) process. Transformation of Tc(VII) to Tc(V) is especially visible for elevated temperature at which a developed electroreduction wave (c1) is observed at −0.05 V. A decrease in the temperature results in shifting of this wave toward lower potentials. It is noteworthy that the second electroreduction wave (c2) is observed almost at the same potential of −0.2 V for all temperatures, which suggests the reversible electrochemical redox reaction of reduced Tc species.

The main product of the pertechnetate reduction is Tc(IV), as the results of hydrodynamic experiments show. A decrease in the temperature of the solution results in an increase in its viscosity and in a decrease in ionic mobility. This is manifested by a decrease of the currents for appropriate CV curves as the temperature decreases. Based on the electrochemical measurements, the generation of dimeric structures of Tc(III/IV), apart from Tc(IV), in ChCl : FA solution cannot be excluded. Electrooxidation of reduced Tc species proceeds through two main

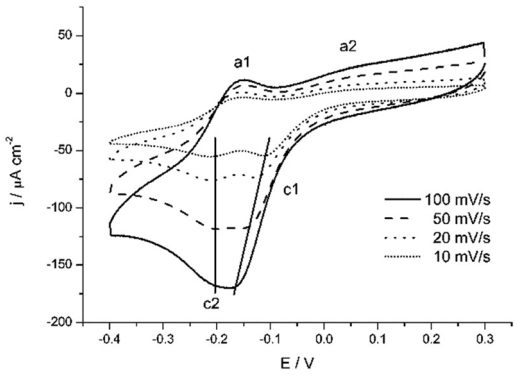

Fig. 4 Cyclic voltammograms recorded with various scan rates for a GC electrode in 1.2 mM $KTcO_4$ + ChCl : FA, T = 25 °C.

steps observed at *ca.* −0.15 V (a1) and above 0 V (a2). The impact of the scan rate on recorded CV curves is shown in Fig. 4. For the lowest scan rate (10 mV s^{-1}), the first reduction wave (c1) is observed at *ca.* −0.12 V. In contrast to the results observed in aqueous solutions,[29] an increase of this parameter results in shifting the potential of the analysed wave toward lower values. This result supports the conclusion from the previous paragraph about electrochemical irreversibility of the first step of the pertechnetate electroreduction. The second electroreduction wave is observed at *ca.* −0.2 V for all analysed cases.

Fig. 5 presents the influence of the impact of Tc concentration on the shape of cyclic voltammogram curves. Especially visible is the formation of the second anodic peak (a2) at higher Tc concentration. Its reduced species in acidic solution may undergo a polymerization process with the generation of Tc–O–Tc chains.[17] As an analogy to the results obtained in aqueous solutions,[38] it seems that at potentials higher than −0.05 V, polymeric forms of Tc, which are especially resistive to oxidation, are electrooxidized to pertechnetates. The second peak current (c2) *vs.* Tc concentration analysis shows their linear relationship (ESI† S6). The separation of the peaks (c2) and (a1) equals *ca.* 60 mV, which supports the conclusion about one-electron reversible reduction of Tc, Tc(v) to Tc(iv). At this point

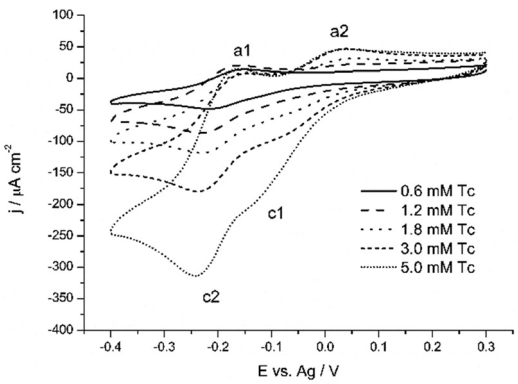

Fig. 5 Cyclic voltammograms recorded in ChCl : FA and various concentrations of $KTcO_4$, scan rate = 50 mV s^{-1}, T = 25 °C.

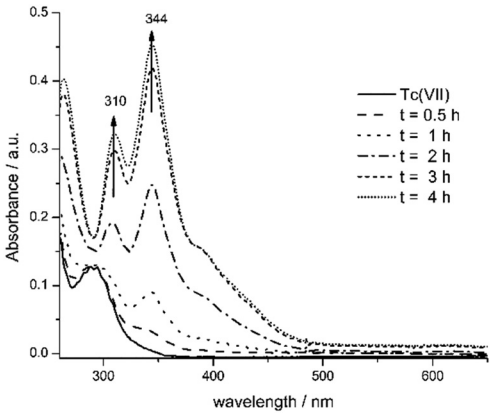

Fig. 6 UV-Vis spectra recorded during chronoamperometric reduction of 0.7 mM $KTcO_4$ in ChCl : FA, E = −0.1 V, T = 25 °C, optical path length – 0.1 cm. Reduced Tc species are indicated at 310 nm and 344 nm.

it should be stressed that description of the pertechnetates electroreduction to Tc(iv) and subsequent oxidation of the latter under stationary conditions cannot be described by any of the commonly known electrochemical mechanisms:[36] simple 3-electron reduction (EEE), electroreduction coupled with a chemical reaction (ECE), disproportionation (EDIS) or reduction of adsorbed species (AE).

Just like in the case of cyclic voltammetry experiments under stationary conditions (see Fig. 3), the results of chronopotentiometric measurements also reveal a multi-path process of Tc(vii) electroreduction (ESI† S7). Two transition times are clearly visible, and this suggests the presence of two separate charge transfer processes. The first process occurs at *ca.* −0.05 V while the second one is observed at −0.2 V. Both potential values are in line with the results of CV measurements (Fig. 3). Fig. 6 shows evolution of UV-vis spectra recorded after potentiostatic reduction of pertechnetates at a potential of −0.1 V and at a temperature of 25 °C. The reduction process leads to the formation of reduced Tc species characterized by the bands with maxima at *ca.* 310 and 344 nm. The longest polarisation

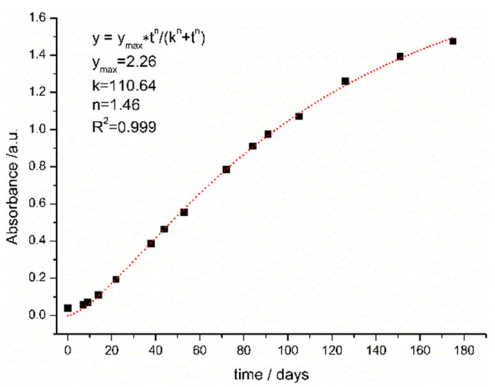

Fig. 7 Time dependence changes in the absorbance at 344 nm observed in 0.34 mM $KTcO_4$ +ChCl : FA, T = 25 °C, optical path length – 1 cm (note: in the original Hill's equation the independent variable is the concentration of reacting compound).[40]

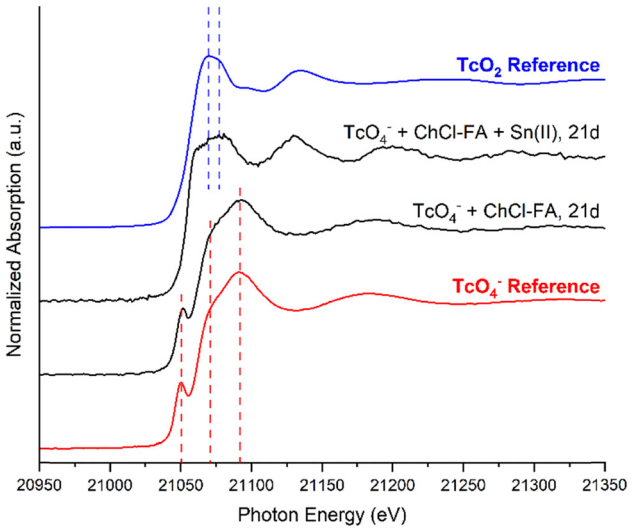

Fig. 8 Tc K-edge XANES spectra measured for aqueous sample solutions containing TcO_4^- and ChCl : FA in the absence of $SnCl_2$ (sample (I), lower line) or in the presence of $SnCl_2$ (sample (II), upper line) after 21 days of equilibration. The TcO_2(am,hyd) (upper, blue line) and TcO_4^- (lower, red line) reference spectra are shown for comparison. These slight changes could potentially be qualitative indications that minor changes (in the oxidation state of Tc) are occurring in solution.

time (4 h) results in a spectrum with a shape similar to that reported for hexachlorotechnetates(IV).[23,39]

An analysis of the spectra excludes generation of oxo-technetium aqueous or formic species. This follows from the absence of respective bands attributed to dimeric Tc ions: $[Tc(\mu\text{-}O)_2Tc]^{4+}$ (λ_{max} = 652 nm[25,26]), $Tc_2O_2(HCOO)_6^{3-}$ (λ_{max} = 652 nm) and $Tc_2O_2(HCOO)_6^{2-}$ (λ_{max} = 530 nm[27]). The low water content in the mixture prevents generation of technetium dioxide. The presence of the latter would be revealed by a significant increase of the absorbance in a broad range of wavelengths. It is worth stressing that TcO_2 is a major product of the pertechnetates electroreduction in low pH aqueous solutions.[17]

Formic acid is a weak reducing agent and could potentially react with Tc(VII). Therefore, additional UV-vis experiments were performed in order to elucidate the importance of this process. A solution containing 0.34 mM $KTcO_4$ + ChCl : FA was tightly sealed in a cuvette and aged at 25 °C for 6 months. Fig. 7 shows the changes in absorbance at 344 nm with time. This wavelength is characteristic of Tc(IV)–Cl species and can be used for tracking the formation of reduced Tc forms. As can be seen, reduction of Tc(VII) by formic acid is very slow at room temperature. Under such conditions, the formation of significant amounts of reduced Tc takes as long as one month. The evolution of the absorbance at 344 nm shown in Fig. 7 is typical for autocatalytic processes described by the Hill-type equation. This suggests that the presence of reduced Tc forms accelerates the reduction of Tc(VII). It is worth noting that autocatalytic processes which involve Tc(VII) were previously reported for aqueous Tc solutions.[16] A similar sigmoidal shape of the absorbance vs time curves was observed during the formation of reduced Tc species in an aqueous TcO_4^- + Na_2S system by German *et al.*[41]

The structure of the Tc species formed during Tc(VII) electrochemical reduction was further elucidated using X-ray absorption spectroscopy. Fig. 8 shows experimentally-measured X-ray absorption near edge structure (XANES) spectra for two samples: sample (I) consisted of a combination of TcO_4^- and ChCl : FA, while sample (II) consisted of this same solution with the addition of $SnCl_2$ as a reducing agent. The UV-vis spectrum of the latter was very similar to those recorded after potentiostatic reduction of Tc(VII) in ChCl : FA solution. It is clear from the comparison to reference spectra that (I), which did not contain $SnCl_2$, was predominantly Tc(VII) after 21 days of equilibration. However, slight differences can be observed between (I) and the Tc(VII) spectrum; the white line peak of (I) was slightly wider than the Tc(VII) reference, and (I) also exhibited a decrease in the pre-edge intensity compared to the reference.

Sample (II) exhibited a white line location similar to the TcO_2(am,hyd) reference spectrum, and also did not show any presence of a pre-peak. As pre-peaks within Tc XANES spectra are characteristic of non-centrosymmetric species, such as

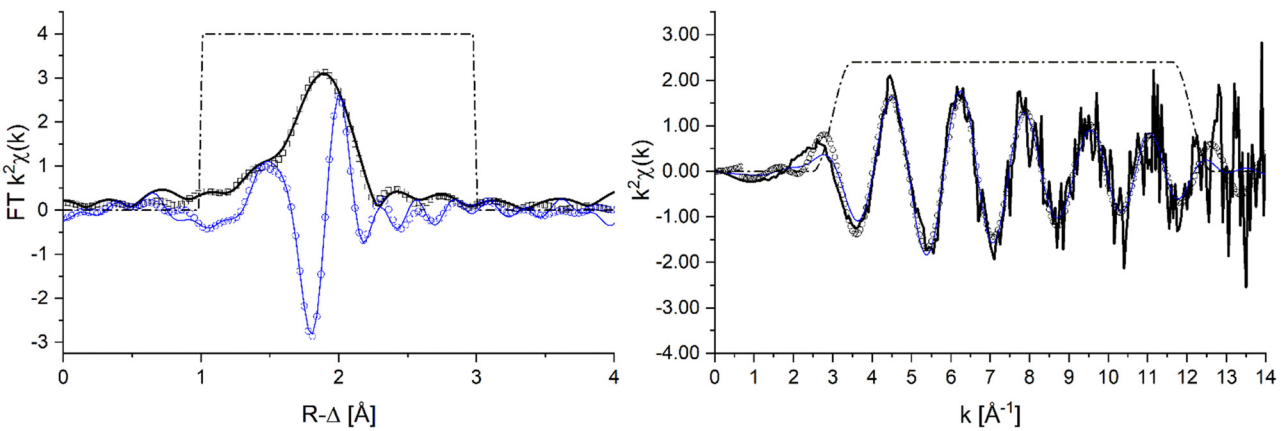

Fig. 9 Tc K-edge EXFAS fit for sample (II), containing TcO_4^-, ChCl : FA, and $SnCl_2$. Left panel: FT magnitude (thick black line), fit magnitude (open black circles), FT real part (thin blue line), and fit real part (blue open triangles); right panel: Fourier filtered data (thick black line), raw data (thin blue line), and back-transformed fit (open black circles). The *R*- and *k*-range fitting windows are represented by dashed lines.

Table 2 Data range and parameters generated by least-squares fitting of the EXAFS spectrum of (II)

Sample	k-Range (Å^{-1}), fit-range (Å)	Path	N	R (Å)	ΔE_0 (eV)	σ^2 (Å^2)	r-Factor (%)
Sample (II)	2.985–12.126, 1.0–3.0	Tc–Cl	5.45	2.36	1.790	0.002	1.05

S_0^2 = 0.95, determined from TcO_4^- reference analysis (fixed no = 4.0). Fit errors: CN: ± 10%, R: 0.01 Å, σ^2: 0.001 Å^2.

would be expected for Tc(v) or Tc(vii), we can conclude from the lack of pre-edge and white line location that Tc was present as the +IV oxidation state in the experimental solution that contained $SnCl_2$. However, significant differences were observed between the TcO_2 reference and the XANES spectrum of (II). Most notably, (II) exhibited a wider white line peak, a shifted first-feature position towards lower photon energy, and larger EXAFS contributions out to further k-range. These observations all combine to indicate that the Tc within the experimental solution obtained an overall different coordination environment than the Tc oxide solid phase. To further investigate this different coordination environment, the Tc K-edge spectrum of (II) was fit using standard least squares techniques. While fitting procedures were attempted using multiple Tc–O, Tc–Cl, or a combination of both Tc–O and Tc–Cl shells, the best results were achieved through fitting the experimental spectrum with a single Tc–Cl coordination shell. Fig. 9 shows the experimental Fourier transformed and Fourier filtered data along with the fitting results, and structural parameters generated from the fit are reported in Table 2. The EXAFS fit exhibited a single Tc–Cl bond distance of 2.36 ± 0.01 Å with a coordination number (N_{Cl}) of 5.45 ± 0.39, which agrees very well with the reported values of 2.36 ± 0.02 and N_{Cl} = 5.0 ± 1.3 for the Tc(iv)–Cl complex $TcCl_6^{2-}$.[42]

D Conclusion

In this work, we describe the physicochemical properties of the mixture of choline chloride (ChCl) with formic acid (FA). Relatively high ionic conductivity and low viscosity make these solutions suitable for electrochemical applications in a wide temperature range. Differential scanning calorimetry revealed that the ChCl : FA solution remains in a liquid state at temperatures as low as −100 °C. Formic acid acts as a very weak reducing agent of Tc(vii) and this reaction is less relevant in a short time scale but becomes important for aged Tc(vii)–ChCl : FA solutions. The electrogeneration of reduced ionic Tc species has been previously observed in strongly acidic solutions (above 1 M H_2SO_4). The present studies clearly show that this process can be carried out in a non-aqueous solution containing a weak carboxylic acid. Opposite to a weak acidic aqueous environment, the presence of choline chloride in formic acid prevents the generation of Tc oxides. Instead, a soluble complex of monomeric Tc(iv) is formed. This process could be beneficial for the synthesis of the desired Tc compounds.

Author contributions

Writing—original draft preparation, investigation, visualization, electrochemical, UV-vis spectroscopic and physicochemical (ChCl : FA) data curation, conceptualization, and methodology: D. P.; XAS data curation, visualization, and draft review: N. D., K. D., X. G.; methodology, review, validation, and supervision: K. C.; conceptualization, methodology, review and editing, and supervision: M. C. All authors have read and agreed to the published version of the manuscript.

Conflicts of interest

There are no conflicts to declare.

Acknowledgements

The contribution of Damian Połomski was realized within Project No POWR.03.02.00-00-I009/17-00 (Operational Project Knowledge Education Development 2014-2020 co-financed by European Social Fund). The KIT Institute for Beam Physics and Technology (IBPT) is acknowledged for the operation of the storage ring, the Karlsruhe Research Accelerator (KARA), and provision of beamtime at the INE and ACT Beamlines operated by the Institute for Nuclear Waste Disposal at the KIT synchrotron light source.

References

1 B. B. Hansen, S. Spittle, B. Chen, D. Poe, Y. Zhang, J. M. Klein, A. Horton, L. Adhikari, T. Zelovich, B. W. Doherty, B. Gurkan, E. J. Maginn, A. Ragauskas, M. Dadmun, T. A. Zawodzinski, G. A. Baker, M. E. Tuckerman, R. F. Savinell and J. R. Sangoro, *Chem. Rev.*, 2021, **121**, 1232–1285.
2 R. Bernasconi, G. Panzeri, A. Accogli, F. Liberale, L. Nobili and L. Magagnin, *Ionic liquids*, ed. S. Handy, IntechOpen: 2017, ch. 11.
3 C. A. Nkuku and J. LeSuer, *J. Phys. Chem. B*, 2007, **111**, 13271–13277.
4 R. Bernasconi, A. Lucotti, L. Nobili and L. Magagnin, *J. Electrochem. Soc.*, 2018, **165**(13), D620–D627.
5 M. Manolova and R. Böck, *Trans. IMF*, 2019, **97**(3), 161–168.
6 F. I. Danilov, D. A. Bogdanov, O. V. Smyrnova, S. A. Korniy and V. S. Protsenko, *J. Solid State Electrochem.*, 2022, **26**, 939–957.
7 A. P. Abbott, G. C. Apper, D. L. Davies, R. K. Rasheed and V. Tambyrajah, *Chem. Commun.*, 2003, 70–71.
8 K. Biernacki, H. K. S. Souza, C. M. R. Almeida, A. L. Magalhães and M. P. Gonçalves, *ACS Sustainable Chem. Eng.*, 2020, **8**, 18712–18728.
9 A. P. Abbott, G. Capper, D. L. Davies, K. J. McKenzie and S. U. Obi, *J. Chem. Eng. Data*, 2006, **51**, 1280–1282.
10 I. M. Pateli, D. Thompson, S. S. M. Alabdullah, A. P. Abbott, G. R. T. Jenkin and J. M. Hartley, *Green Chem.*, 2020, **22**, 5476–5486.

11 D. Połomski, P. Garbacz, K. Czerwinski and M. Chotkowski, *J. Mol. Liq.*, 2021, **327**, 114820.
12 R. Gupta, B. G. Vats, A. K. Pandey, M. K. Sharma, P. Sahu, A. K. Yadav, S. Musharaf Ali and S. Kannan, *J. Phys. Chem. B*, 2020, **124**(1), 181–189.
13 J. M. Bonnerot, V. Broudic, M. Phélip, C. Jégou, F. Varaine, X. Deschanels, M. F. Arnoux and J. L. Faugère, *J. Nucl. Radiochem. Sci.*, 2005, **6**(3), 287–290.
14 U. Mazzi, R. Schibli, H.-J. Pietzsch, J.-U. Künstler and H. Spies, in *Technetium in medicine in Technetium-99m pharmaceuticals*, ed. I. Zolle, Springer, 2007, pp. 7–58.
15 A. Duatti, *Chapter 1. Role of ^{99m}Tc in diagnostic imaging in Technetium-99m Radiopharmaceuticals: Status and Trends, IAEA Radioisotopes And Radiopharmaceuticals Series No. 1*, IAEA, 2009, pp. 7–18.
16 T. J. Kemp, S. A. M. Thyera and P. D. Wilson, *J. Chem. Soc., Dalton Trans.*, 1993, 2601–2605.
17 M. Chotkowski and A. Czerwiński, in *Electrochemistry of technetium, serie*, ed. F. Scholtz, Monographs in Electrochemistry, Springer, 2021.
18 N. Vongsouthi, PhD thesis, Université de Nantes, UFR Sciences et Techniques, 2009.
19 M. Chotkowski, B. Wrzosek and M. Grdeń, *J. Electroanal. Chem.*, 2018, **814**, 83–90.
20 F. Poineau, P. F. Weck, B. P. Burton-Pye, I. Denden, E. Kim, W. Kerlin, K. E. German, M. Fattahi, L. C. Francesconi, A. P. Sattelberger and K. R. Czerwinski, *Dalton Trans.*, 2013, **42**(13), 4348–4352.
21 M. Zegke, D. Grçdler, M. R. Jungfer, A. Haseloer, M. Kreuter, J. M. Neudörfl, T. Sittel, Ch. M. James, J. Rothe, M. Altmaier, A. Klein, M. Breugst, U. Abram, E. Strub and M. S. Wickleder, *Angew. Chem., Int. Ed.*, 2022, **61**, e202113777.
22 L. Vichot, M. Fattahi, C. Musikas and B. Grambow, *Radiochim. Acta*, 2003, **91**(5), 263–272.
23 P. Rajec and F. Macášek, *J. Inorg. Nucl. Chem.*, 1981, **43**, 1607–1609.
24 F. Poineau, A. P. Sattelberger, S. D. Conradson and K. R. Czerwinski, *Inorg. Chem.*, 2008, **47**(6), 1991–1999.
25 C. M. Kennedy and T. C. Pinkerton, *Appl. Radiat.*, 1988, **39**(2), 1159–1165.
26 C. M. Kennedy and T. C. Pinkerton, *Appl. Radiat.*, 1988, **39**(11), 1167–1177.
27 A. Maslennikov, M. Masson, V. Peretroukhine and M. Lecomte, *Radiochim. Acta*, 1999, **84**, 53–58.
28 V. V. Kuznetsov, M. A. Volkov, K. E. German, E. A. Filatova, O. A. Belyakova and A. L. Trigub, *J. Electroanal. Chem.*, 2020, **869**, 114090.
29 M. Chotkowski and A. Czerwiński, *Electrochim. Acta*, 2012, **76**, 165–173.
30 J. Rothe, M. Altmaier, R. Dagan, K. Dardenne, D. Fellhauer, X. Gaona, E. C. González-Robles, M. Herm, K. O. Kvashnina, V. Metz, I. Pidchenko, D. Schild, T. Vitova and H. Geckeis, *Geosciences*, 2019, **9**(2), 91–113.
31 J. Rothe, S. Butorin, K. Dardenne, M. A. Denecke, B. Kienzler, M. Löble, V. Metz, A. Seibert, M. Steppert, T. Vitova, C. Walther and H. Geckeis, *Rev. Sci. Instrum.*, 2012, **83**(4), 043105.
32 B. Ravel and M. Newville, *J. Synchrotron Radiat.*, 2005, **12**(Pt 4), 537–541.
33 E. V. Johnstone, F. Poineau, P. M. Förster, L. Ma, T. Hartmann, A. Cornelius, D. Antonio, A. P. Sattelberger and K. R. Czerwinski, *Inorg. Chem.*, 2012, **51**(15), 8462–8467.
34 J. Hietala, A. Vuori, P. Johnsson, I. Pollari, W. Reutemann and H. Kieczka, *Formic acid, Ulmann's encyclopedia of industrial chemistry*, 2016.
35 A. P. Abbott, D. Boothby, G. Capper, D. L. Davies and R. K. Rasheed, *J. Am. Chem. Soc.*, 2004, **126**(29), 9142–9147.
36 A. J. Bard and F. R. Faulkner, Electrochemical methods, *Fundamentals and applications*, Wiley, 2nd edn, 2000.
37 Y. A. Elhamarnah, M. Nasser, H. Qiblawey, A. Benamor, M. Atilhan and S. Aparicio, *J. Mol. Liq.*, 2019, **277**, 932–958.
38 M. Chotkowski and A. Czerwiński, *J. Radioanal. Nucl. Chem.*, 2014, **300**, 229–234.
39 S. Ben, K. M. Fattahi, C. Musikas, R. Revel and J. Ch. Abbé, *Radiochim. Acta*, 2000, **88**(1), 567–571.
40 J. N. Weiss, *FASEB J.*, 1997, **11**, 835–841.
41 K. E. German, A. A. Shiryaev, A. V. Safonov, Y. A. Obruchnikova, V. A. Ilin and V. E. Tregubova, *Radiochim. Acta*, 2015, **103**(3), 199–203.
42 N. J. Hess, Y. Xia, D. Rai and S. D. Conradson, *J. Solution Chem.*, 2004, **33**(2), 199–226.